Communication: Inflection in the pressure dependent conductivity of the protic ionic liquid C8HIM NTf2

Inflection in the pressure dependent conductivity of the protic ionic liquid C_8HIM NTf_2

Erik Thoms,[1, a)] Zaneta Wojnarowska,[1, b)] Peter Goodrich,[2] Johan Jacquemin,[2] and Marian Paluch[1, c)]
[1)] *Silesian Center for Education and Interdisciplinary Research, 75 Pulku Piechoty 1A, 41-500 Chorzow, Poland.*
[2)] *The QUILL Research Centre, School of Chemistry and Chemical Engineering, Queen's University of Belfast, Stranmillis Road, Belfast BT9 5AG, United Kingdom.*

(Dated: 4 May 2017)

Temperature and pressure dependent broadband dielectric measurements were performed on the protic ionic liquid C_8HIM NTf_2 over a frequency range from 0.1 Hz to 1 MHz. The temperature dependence of the inverse dc-conductivity exhibits the superarrhenius like behavior typical for glass forming materials. However, in the pressure dependence both slower and faster than exponential developments occur, resulting in an inflection in the corresponding curves. The experimental data were successfully fitted with a model incorporating both features. While similar transitions have been observed in the pressure dependent viscosity or structural relaxation times, this is the first time such behavior is reported in the conductivity.

In the past decade, the interest in researching ionic liquids (ILs) has risen tremendously. This can be ascribed to their many potential areas of application, including, *e.g.*, the usage as biosolvents, as transport medium for electrodeposition or as electrolytes in energy storage devices[1]. The base for this widespread potential can be found within the unique properties many ILs have, like extremely high vapor pressure, good thermal, chemical, and voltage stability or high solubility with many substances. Additionally, being salts with a low melting point, usually defined to be above room temperature[1] or 100 °C[2], they have high ionic conductivity, which is essential for energy applications. Due to the mostly organic nature and thus the huge variability of possible cations and, to a lesser degree, anions, a vast amount of ILs exist.

On the other hand, from a physical point of view, many ILs are typical glass formers, *i.e.* they tend to supercool and form amorphous solids rather than crystals upon cooling. Like many glass formers, they exhibit superarrhenius like temperature dependence of the viscosity η, which is usually well described by the empirical Vogel-Fulcher-Tammann-Hesse equation (VFTH equation)[3–5]:

$$\eta(T) = \eta_\infty \times \exp\left(\frac{DT_{VF}}{T - T_{VF}}\right) \tag{1}$$

where T is the absolute temperature, η_∞ is the viscosity for very high T and T_{VF} is the Vogel-Fulcher temperature. The strength parameter D quantifies fragility, *i.e.*, the divergence from ideal Arrhenius behavior. Similar expressions exist to describe the T-dependence of the dc-conductivity σ_{dc} and the structural relaxation time. Many ILs seem to follow a fractional Walden rule, *i.e.* $\Lambda\eta^\alpha = \text{const.}$ (with the molar conductivity Λ and the constant exponent $0 < \alpha < 1$)[6]. For so-called aprotic ILs, α usually is close to one and depends mainly on the degree of ion dissociation[7,8]. This implies that the inverse conductivity $1/\sigma_{dc}$ has the same temperature dependence as the viscosity. On the other hand, protic systems can exhibit pronounced deviations from this behavior, based on the presence of multiple conductivity mechanisms[9].

Another way to generate a vitreous state is to increase the pressure p and therefore to limit free volume of the molecules. The relationship between the influences of pressure and temperature on the glass transition, and the differences therein, are important aspects for the understanding of this process. A systematic analysis of both aspects allows to separate the effects on local motion provided by molecular packing and by available energy[10]. It is very interesting that compared to the temperature dependence of σ_{dc} or η, the pressure evolution of these variables is much more complex. In general, the viscosity rises with pressure. Close to the glass transition, this increase is faster than exponential and can be described by a pressure equivalent of the VFTH-law[11],

$$\eta(p) = \eta_0 \times \exp\left(\frac{C_F p}{p_\infty - p}\right) \tag{2}$$

where η_0 is the viscosity for very low pressures, C_F is a pressure analogue to D and p_∞ is the divergence pressure. By contrast, in the normal liquid state, *i.e.*, for low pressures or high temperatures, a slower than exponential behavior is observed for many materials[12]. This leads to a clear deviation from the model presented above and a perturbation of the fitting parameters. To model $\eta(p)$ in this range, the McEwen equation

$$\eta(p) = \eta_0 \times \left(1 + \frac{\alpha_0}{q}p\right)^q \tag{3}$$

can be used[13]. Here, q represents the McEwen exponent, while the McEwen parameter α_0 determines the slope at

[a)] erik.thoms@smcebi.edu.pl; Institute of Physics, University of Silesia, Uniwersytecka 4, 40-007 Katowice, Poland
[b)] Institute of Physics, University of Silesia, Uniwersytecka 4, 40-007 Katowice, Poland; Chemical Sciences Division, Oak Ridge National Laboratory, Oak Ridge, Tennessee 37831, USA
[c)] marian.paluch@us.edu.pl; Institute of Physics, University of Silesia, Uniwersytecka 4, 40-007 Katowice, Poland

$p = 0$. With a combination of both equations, as suggested by Bair[13], usually the whole pressure dependency of the viscosity is described rather well:

$$\eta(p) = \eta_0 \times \left(1 + \frac{\alpha_0}{q} p\right)^q \times \exp\left(\frac{C_F p}{p_\infty - p}\right) \qquad (4)$$

Interestingly, to our knowledge no reports of slower than exponential behavior of the inverse conductivity have been published so far.

In this paper we investigate the ion dynamics of the protic ionic liquid C_8HIM NTf_2 over a wide T and p range. In the $\sigma(p)$ data, we observed McEwen-like behavior of $1/\sigma_{dc}$ at low pressures, while at higher pressures faster than exponential behavior is exhibited. The data was fitted according to the hybrid model (Eq. 4) and analyzed in regards of the activation volume, illustrating the presence of an inflection point in the curves.

The C_8HIM NTf_2 (1-Octylimidazolium Bis(trifluoromethylsulfonyl)imide) was synthesized and purified at the QUILL Research Centre at Queens University Belfast. Details are available in the supplementary material. For the high pressure dielectric measurements, the sample was filled in a stainless steel plate capacitor with 100 µm silica spacers. The capacitor was covered in a Teflon capsule, which was then placed in the high pressure chamber. Hydrostatic pressure was applied via a non-polar transmitting liquid (silicon oil). An Alpha-A Analyzer (Novocontrol) was used to perform the dielectric measurements at a frequency range from 0.1 Hz to 1 MHz with a excitation voltage of 0.5 V, assuming a standard uncertainty of the conductivity of 1 mS/cm. The pressure was measured with a Nova Swiss tensometric pressure meter (resolution 0.1 MPa). For the temperature control, a Weiss fridge was employed with an uncertainty of 0.1 K.

The real part of the conductivity σ' of C_8HIM NTf_2 is shown in Fig. 1 in dependence of the frequency ν for different values of the pressure p at a constant temperature of 273 K. The dc-conductivities can be observed at frequency-independent plateaus, *e.g.*, for the 350 MPa curve between 100 Hz and approximately 10 kHz. At higher frequencies, the presence of intrinsic relaxations is suggested by a pronounced pressure dependence of sigma, visible for curves with $p \geq 150$ MPa. Frequencies below that of the observed plateau in σ' exhibit a strong decrease of the conductivity with decreasing ν. This effect can be attributed to the well-known blocking electrodes effect, *i.e.*, the build-up of a thin, insulating layer at the electrodes. Compression of the sample leads to higher viscosity and thus to reduced ion mobility in the liquids. As an effect, both the intrinsic and the surface processes shift to lower frequencies with higher pressure. Additionally, it can be seen that σ_{dc} is decreasing by more than two decades from 9×10^{-5} S/cm to 3×10^{-7} S/cm when p increases from 12 MPa to 400 MPa.

One method to evaluate dynamic processes is the dielectric modulus representation[14]. Its significance is still controversially discussed, however it allows for identification of the charge transport connected with intrinsic relaxation processes, while the influence of electrode polarisation is suppressed leading to frequent usage of this representation in the characterisation of ILs. From the maximum of the imaginary part of the dielectric modulus M'' (not shown), the so-called conductivity relaxation time $\tau_\sigma = 1/2\pi f(M''_{max})$ can be determined. For example, at 273 K and 400 MPa, τ_σ reaches 6×10^{-6} s and diminishes with pressurisation and with cooling.

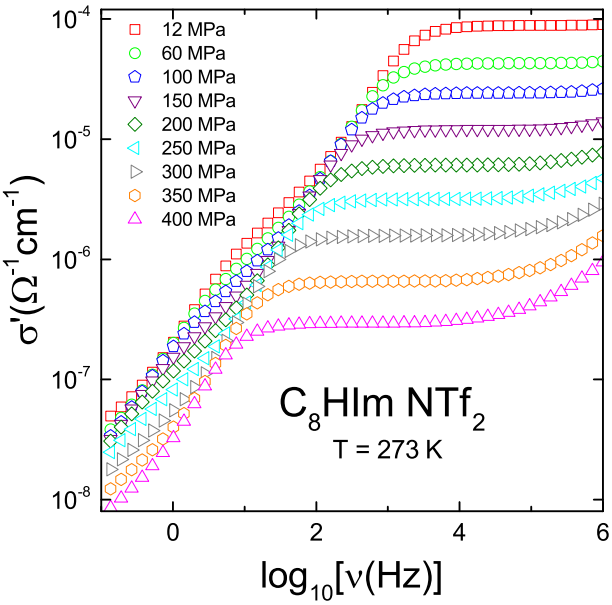

FIG. 1. Frequency dependency of the conductivity of C_8HIM NTf_2 for selected pressures. The dc-conductivity is observed as a plateau at elevated frequencies.

To further examine the decrease of σ with pressure, the inverse dc-conductivity is presented as a function of p in Fig. 2 for different temperatures. It can clearly be seen that for $p < 300$ MPa the 293 K curve is concave against the p-axis, *i.e.*, $1/\sigma_{dc}$ develops slower than exponential with p. In contrast, faster than exponential behavior is observed at higher pressures, indicated by the stronger increase in $1/\sigma_{dc}$. This leads to an inflection in the curves. Whether this feature is reflected in the pressure dependent viscosity for C_8HIM NTf_2 is not clear so far. However, a similar behavior can be seen in $\eta(p)$ for many molecular liquids[15,16] and some ionic liquids[17], even though the concave progression at low pressures is not necessarily incorporated in the models used in these reports. This inflection might arise from a non linearity of the volume with a change of pressure[18]. It has also been attributed to the pressure dependences of the compressibility and of the apparent activation energy at constant volume[16]. The hybrid model (Eq. 4) is used to account for both the faster and the slower than exponential behavior and describes the measured data reasonably well (lines in Fig. 2), assuming a temperature independent pressure-related fragility (*i.e.*, $C_F = \text{const.}$)[19]. Be-

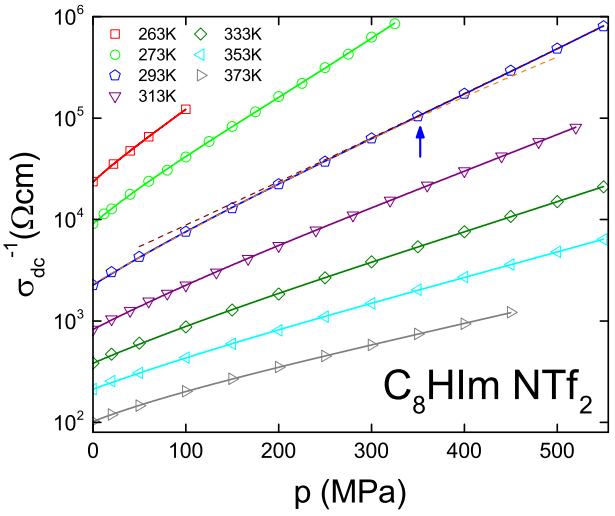

FIG. 2. Pressure dependency of the dc conductivity of C_8HIM NTf_2 for seven isotherms. The lines represent fits with the hybrid model (Eq. 4). Exemplary for 293 K, the inflection point is marked by an arrow and fits according to equations 2 and 3 in the corresponding regimes are shown (brown and orange dashed lines, respectively).

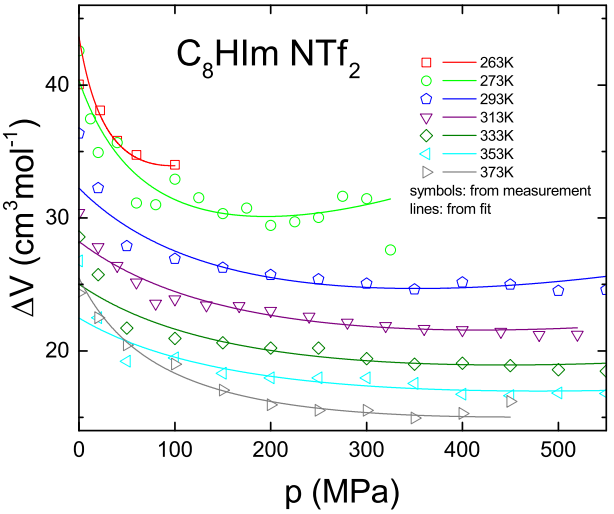

FIG. 3. Pressure dependent activation volume of C_8HIM NTf_2. The lines are calculated from the fits shown in Fig. 2. Error bars are smaller than the symbol size.

sides, it can be noted that due to improved ion mobility the conductivity rises when T is increasing, which is in agreement with Eq. 1. For example, at ambient pressure and $T = 263\,\mathrm{K}$, σ_{dc} is approximately 4×10^{-5} S/cm, while at 373 K a value close to 10^{-2} S/cm is reached. Extrapolation of the modulus data for $T = 273\,\mathrm{K}$ and 293 K yields relaxation times on the order of 10^{-8} s at the inflection point ($p \approx 200$ and 350 MPa, respectively).

The presence of the inflection point becomes more obvious when the $\sigma_{dc}(p)$ data are analyzed in terms of the activation volume parameter

$$\Delta V(p) = RT \times \left(\frac{\partial \log(\sigma_{dc}^{-1})}{\partial p} \right) \tag{5}$$

as presented in Fig. 3, where R is the universal gas constant. $\Delta V(p)$ is a measure of the local volume needed for transversal ion movement and has a constant value for Arrhenius like behavior. Consequently, slower than exponential pressure dependence of $1/\sigma_{dc}$ is indicated by a negative slope, while faster than exponential behavior correlates to a positive slope. Therefore the inflection point corresponds to the minimum in ΔV, clearly visible, e.g., for the 273 K data at a pressure of approximately $p_i = 200$ MPa. With rising temperature, the point shifts to higher pressures. The shift is fast initially, but slows down significantly at high T. Measurements performed by Cook *et al.*[15] show inflection points in the viscosity of glycerol and dibutyl phthalate (DBP) over a temperature range from 273 K to 398 K. While the temperature dependence of p_i for glycerol is similar to C_8HIM NTf_2, DBP exhibits a more linear $p_i(T)$-behavior. It could be speculated that this observation is connected to the strong H-bonding in both glycerol and C_8HIM NTf_2, which is absent in dibutyl phthalate. Besides, it should be noted that the inflection in glycerol is observed at higher pressure (*e.g.* 1.3 GPa at 296 K) than in DBP and C_8HIM NTf_2 (360 respectively 352 MPa at similar T).

High pressure broadband dielectric spectroscopy was performed on the protic ionic liquid C_8HIM NTf_2 for different temperatures. For the first time, we could observe a transition between slower than exponential and Vogel-Fulcher-like pressure dependence of the dc-conductivity, similar to the behavior reported in pressure dependent viscosity and relaxation times in other materials[15–17]. The measured data was fitted with the hybrid model suggested by Bair for $\eta(p)$ (Eq. 4) over the whole pressure range. Since the conductivity is a key property for many potential applications of ionic liquids, *e.g.*, for electrolytes in energy storage devices, the sighting of such behavior in a protic IL is highly interesting, as it allows for a more thorough prediction. Additionally, this might help determining the physical mechanisms leading to the inflection in the pressure dependence of different properties.

Details of the synthesis and purification of C_8HIM NTf_2 are available in the supplementary material.

The authors thank J. Knapik-Kowalczuk and B. Blanchard for performing parts of the dielectric measurements. Z.W. and M.P. are deeply grateful for the financial support by the National Science Centre within the framework of the Opus8 project (Grant DEC-2014/15/B/ST3/04246).

[1] M. Armand, F. Endres, D. R. MacFarlane, H. Ohno, and B. Scrosati, Nature Materials **8**, 621 (2009).

[2]H. Weingartner, Angewandte Chemie International Edition **47**, 654 (2008).
[3]H. Vogel, Physikalische Zeitschrift **22**, 645 (1921).
[4]G. S. Fulcher, Journal of the American Ceramic Society **8**, 339 (1925).
[5]G. Tammann and W. Hesse, Zeitschrift fuer anorganische und allgemeine Chemie **156**, 245 (1926).
[6]W. Xu, E. I. Cooper, and C. A. Angell, Journal of Physical Chemistry B **107**, 6170 (2003).
[7]D. R. MacFarlane, M. Forsyth, E. I. Izgorodina, A. P. Abbott, G. Annat, and K. Fraser, Physical Chemistry Chemical Physics **11**, 4962 (2009).
[8]C. Schreiner, S. Zugmann, R. Hartl, and H. J. Gores, Journal of Chemical & Engineering Data **55**, 4372 (2010).
[9]Z. Wojnarowska and M. Paluch, Journal of Physics: Condensed Matter **27**, 073202 (2015).
[10]G. Floudas, M. Paluch, A. Grzybowski, and K. Ngai, *Molecular Dynamics of Glass-Forming Systems* (Springer Berlin Heidelberg, 2011).
[11]M. Paluch, Z. Dendzik, and S. J. Rzoska, Physical Review B **60**, 2979 (1999).
[12]S. Bair, L. Martinie, and P. Vergne, Tribology Letters **63**, 37 (2016).
[13]S. Bair, High Temperatures – High Pressures **44**, 415 (2015).
[14]P. B. Macedo, C. T. Moynihan, and R. Bose, Phys. Chem. Glasses **13**, 171 (1972).
[15]R. L. Cook, H. E. King, C. A. Herbst, and D. R. Herschbach, The Journal of Chemical Physics **100**, 5178 (1994).
[16]R. Casalini and S. Bair, The Journal of Chemical Physics **128**, 084511 (2008).
[17]F. M. Gaciño, M. J. Comuñas, T. Regueira, J. J. Segovia, and J. Fernández, The Journal of Chemical Thermodynamics **87**, 43 (2015).
[18]C. A. Herbst, R. L. Cook, and H. E. K. Jr, Nature **361**, 518 (1993).
[19]M. Paluch, S. Hensel-Bielowka, and J. Ziolo, The Journal of Chemical Physics **110**, 10978 (1999).

Experimental Section

Chemicals

Paraformaldehyde (crystalline reagent grade), glyoxal trimer dihydrate (<97 %), *n*-octylamine (99.5 %), ammonium carbonate (reagent grade) and 35-37wt% hydrochloric acid were purchased from Sigma-Aldrich and used as received. All solvents used were HPLC grade purchased from Riedel de Haën. Lithium bis[(trifluoromethyl)sulfonyl]imide was purchased from 3M (> 98 %).

^{1}H and ^{13}C NMR spectra were recorded at 20 °C on a Bruker Avance DPX spectrometer at 300 MHz and 75 MHz, respectively and are reported herein in Figs. S1 and S2 of the electronic supporting information (ESI). Chemical shifts are given in ppm downfield from TMS.

Synthesis of 1-octylimidazole

To a 200 cm^3 round-bottom flask was added 2.73 g (91 mmol) of paraformaldehyde and 20 cm^3 of methanol. After cooling to 0-5 °C, there was added, in order, 11.15 g (86 mmol) *n*-octylamine, 10 cm^3 methanol, 4.10 g (43 mmol) ammonium carbonate, 10 cm^3 methanol, 6.08 g (29 mmol) trimeric glyoxal dihydrate and 15 cm^3 methanol. The reaction was stirred overnight at room temperature. A small aliquot was removed for NMR analysis. Volatiles were removed under reduced pressure and the reaction mixture was vacuum distilled to yield 8.17 g (48 %) of 1-octylimidazole, b.p. 145 °C. 9 mm Hg.

^{1}H NMR (300 MHz, $CDCl_3$): δ (ppm) 7.65 (s, 1H), 7.08 (s, 1H), 6.93 (s, 1H), 3.95 (t, J = 7.2 Hz, 2H), 1.79 (m, 2H), 1.51 – 1.29 (m, 10H), 0.85 (t, J= 6.9Hz, 3H).

Synthesis of 1-octylimidazolium bis[(trifluoromethyl)sulfonyl]imide

A mixture of 1-octylimidazole (6.89 g, 0.035 mol) was dissolved in deionised water (20 cm^3) and cooled in an ice bath. To this solution was added slowly dropwise hydrochloric acid solution (3.75 g, 0.038 mol). The reaction mixture was stirred for a further hour.

A solution of lithium bis[(trifluoromethyl)sulfonyl]imide (11.48 g, 0.040 mol) in distilled water (20 cm^3) was added drop-wise to the rapidly stirred solution. After one hour dichloromethane (50 cm^3) was added to the biphasic reaction mixture and allowed to stir under ambient conditions overnight. The organic layer was then extracted and washed with distilled water (20 cm^3) repeatedly five times. The organic layer was then dried *in vacuo* to give the product as an off-white liquid 15.86g, < 98% yield.

^{1}H NMR (300 MHz, $CDCl_3$) δ 12.32 (s, 1H), 8.42 (s, 1H), 7.37 (s, *1*H), 7.28 (s, *1*H), 4.18 (t, *J* = 7.4 Hz, 2H), 1.88 (br s, 2H), 1.29 (m, 10H), 0.87 (t, *J* = 6.3 Hz, 6H). ^{13}C NMR (75 MHz, $CDCl_3$) δ 134.77 (s), 126.48 (s), 122.22 (s), 121.73 (s), 117.97 (s), 113.72 (s), 50.10 (s), 31.99 (s), 30.56 (s), 29.25 (s), 26.50 (s), 22.91 (s), 14.35 (s). CHNS calc. C 33.84, H 4.59, N 9.11, S 13.9; exp C 33.53, H 4.49, N 8.89, S 13.01

Chemical characterization

Prior to any measurements the IL was dried under high vacuum (2 x 10^{-3} mbar) for 48 h at 343.15 K. The water content in ILs was analyzed by means of a coulometric Karl-Fischer titration using an 899 Coulometer (Metrohm) with an accuracy better than 10 ppm (see Table S1). To avoid further contamination with moisture from the atmosphere, the IL was then stored in a glovebox under an Ar atmosphere with a moisture content below 3 ppm. Microanalysis, chloride and lithium content were then performed by Analytical Services at Queen's University, Belfast to confirm the high purity of the sample which is close to 99.4 mol%.

Ionic Liquid	Purity Mol%	Mw $gmol^{-1}$	H_2O ppm	Li ppm	Cl ppm
C_8Him NTf_2	>99.4	461.44	58	39	22

Table S1. Purity, molecular weight, water, lithium and chloride content in the C_8Him NTf_2

Figure S1. ^{1}H-NMR of 1-octylimidazolium bis[(trifluoromethyl)sulfonyl]imide

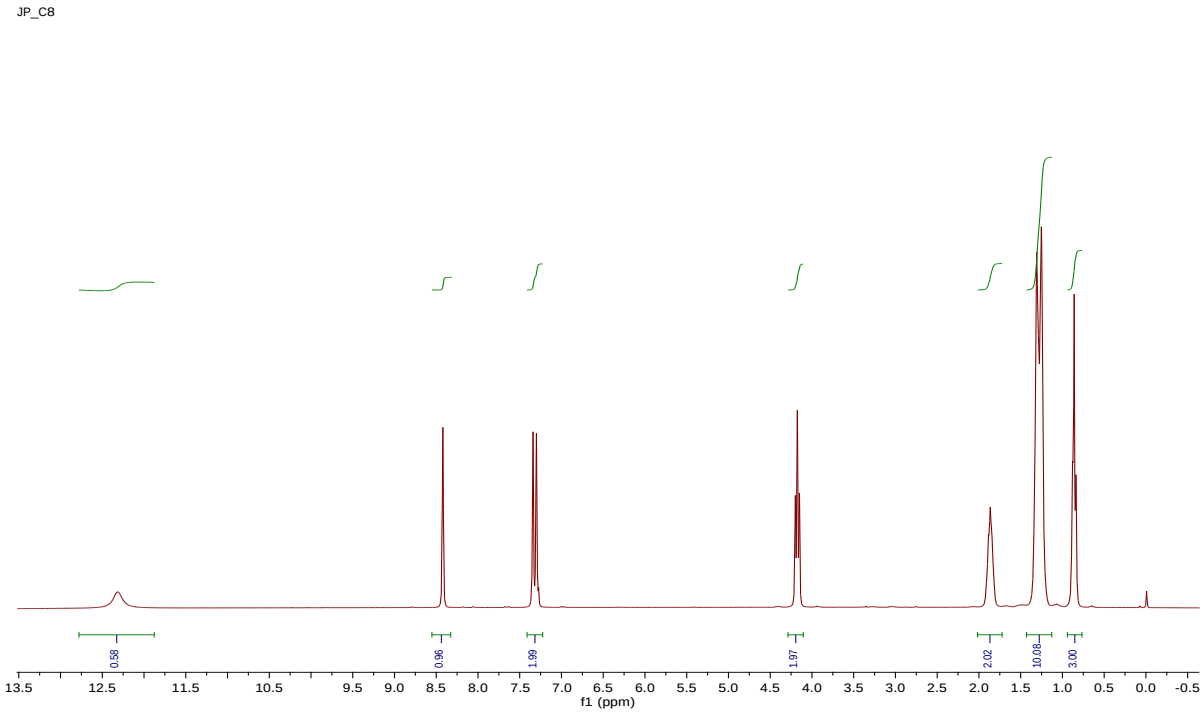

Figure S2. ^{13}C-NMR of 1-octylimidazolium bis[(trifluoromethyl)sulfonyl]imide